3.0 EXPERIMENTAL MATERIALS AND METHODS

In this section are summarized the functional description and physical attributes of the ICET test apparatus, the ICET experimental plan and test matrix to provide context for the results of Test #1, several of the analytic methods that were applied for daily monitoring and sample analysis, and the QA program that is being followed during execution of the ICET series.

3.1 Chemical Test Apparatus Functional Description

The test apparatus was designed to meet the functional requirements of Ref. 2. Functional aspects of the test apparatus that meet those requirements are discussed as follows.

1. The central component of the system is a test tank. The test apparatus was designed to preclude the settling of solids in the test piping.

2. The test tank is capable of maintaining both a liquid and vapor environment, as would be expected in containment post-LOCA.

3. The test loop is capable of controlling the liquid temperature at 140°F within a range of ±5°F.

4. The system is capable of circulating water at flow rates that simulate spray flow rates per unit area of containment cross section.

5. The test tank provides for water flow over submerged test coupons, which is representative of containment pool fluid velocities expected at plants.

6. Piping and related isolation valves were provided such that a section of piping can be isolated without interrupting performance of the test.

7. The pump discharge line was split in two, with one branch directed to the spray header located in the vapor space inside the tank and the other branch returning to the liquid side of the tank. Each branch was provided with an isolation valve and flow meter.

8. A flow meter was provided in the recirculation piping.

9. The pump circulation flow rate is controlled at the pump discharge to be within ±5% of the flow required to simulate fluid velocities in the tank. Flow is controlled manually.

10. The tank accommodates a rack of immersed sample coupons, including the potential reaction constituents identified in the test plan.

11. The tank also accommodates six racks of sample coupons that are exposed to a spray of liquid that simulates the chemistry of a containment spray system. Provision was made for visual inspection of the spray rack.

12. The tank provides for sufficient space between the test coupons so as to preclude galvanic interactions among the coupons. The different metallic test coupons are electrically isolated from each other and the test stand to prevent galvanic effects resulting from metal-to-metal contact between specimens or between the test tank and the specimens.

13. The fluid volumes and sample surface areas were based on scaling considerations that relate the test conditions to actual plant conditions.

14. All components of the test loop were made of corrosion-resistant material (for example, SS for metallic components).

The as-built test loop consists of a test tank, a recirculation pump, 2 flow meters, 10 isolation valves, and pipes for connecting the major components, as shown schematically in Figure 1. Figure 2 and Figure 3 provide photographs of the test loop and the data acquisition system, respectively.

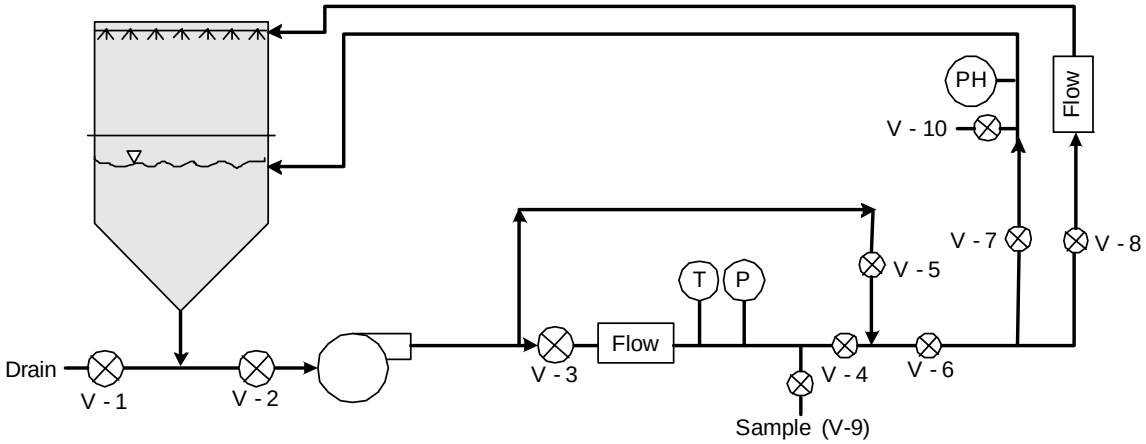

Figure 1. Test loop process flow diagram.

Figure 2. Photograph of the test loop.

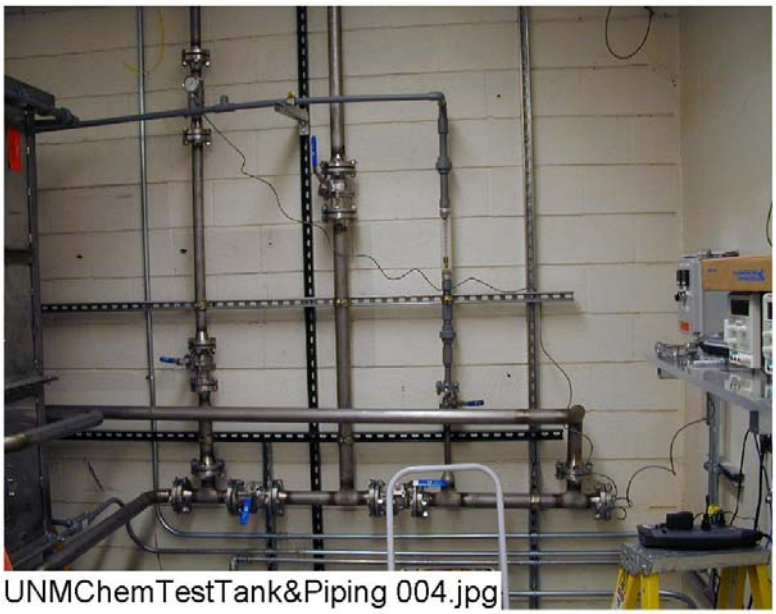

Figure 3. Photograph of the data acquisition system.

3.2 Chemical Tank Assembly and Circulation Details

3.2.1 Materials

The tank, piping, and components were designed of materials that are chemically resistant to a mixture of reverse-osmosis (RO)-treated water, sodium hydroxide (NaOH), trisodium phosphate (TSP), lithium hydroxide (LiOH), hydrochloric acid (HCl), and boric acid in a pH range of 7.0 to 12.0 and a temperature of 140°F. Only one pH control chemical, either NaOH (resulting in a pH of approximately 10) or TSP (resulting in a pH of approximately 7), is used in a given test. The tank is constructed of type 304 SS, with polycarbonate view windows and Goretex® gaskets. The bottom portion of the tank is constructed of 1/8-in.-thick sheet steel reinforced with 1/4-in.-thick by 2-in.-wide angle iron. The upper portion of the tank is constructed of 1/16-in.-thick sheet steel with 1/4-in.-thick by 2-in.-wide angle iron supports. The lid is 1/16-in.-thick sheet steel with 1/4-in.-thick by 2-in.-wide angle iron. One polycarbonate window with Goretex® gaskets is located in the bottom tank section, the top tank section, and the tank lid, for a total of three observation ports.

SS was used for the circulation piping to eliminate the possibility of chemical leaching from the material into the solution. SS also was chosen for the recirculation pump, tank internals, and instruments to ensure that no leaching occurred. To facilitate the construction and assembly of the flow path from the recirculation piping to the spray nozzles, a different material, chlorinated polyvinyl chloride (CPVC) piping, was chosen.

Although leaching from the SS was not an issue, some of the other materials could not be guaranteed against leaching based only on their material descriptions. Thus, separate leaching tests were conducted with bench-scale experiments. CPVC pipe and the solvent used to connect fittings were soaked in a solution of the test chemicals for five days at 70°C. The solution was then tested; results indicated that the level of chloride (the element that might be expected to leach) was not detectable. A secondary concern was whether the CPVC would absorb chemicals, notably boron or sodium. The samples were tested, and results indicated only trace amounts of boron and sodium.

Similarly, the Goretex® gasket material was tested for possible leaching in the test solution chemistry. Chloride and silica are the two elements that could possibly leach from the gasket material. It was found that the scaled amount that did leach was two orders of magnitude less than what was expected from the test additives and fiberglass insulation.

Thus, it was concluded that the test apparatus materials would not contribute chemically to the test solution in concentrations that would impact the test results.

3.2.2 Tank Sizing

The tank is designed to hold 250 gal. of chemical solution, with 2 to 3 inches between the top of the water level and the top half of the tank. The bottom half of the tank is designed to accommodate 250 gal. of solution, a single 60-coupon rack, and mesh cassettes containing 4 ft^3 of fiberglass insulation. The upper portion of the tank is designed to accommodate 6 coupon racks, each containing up to 60 coupons. The tank is nominally 4 ft × 4 ft × 6.6 ft in height, as shown in Figure 4.

Figure 4 through Figure 8 present photographs of the ICET tank, the cover lid, and the internal components, which include the top and bottom angle irons for supporting the racks, the distribution headers, the heaters, the thermocouples, and the spray nozzles.

Figure 4. External view of the ICET tank.

Figure 5. The distribution header, heaters, and thermocouples inside the lower tapered reservoir of the ICET tank.

Figure 6. The top and bottom angle irons for supporting coupon racks in the upper section of the ICET tank.

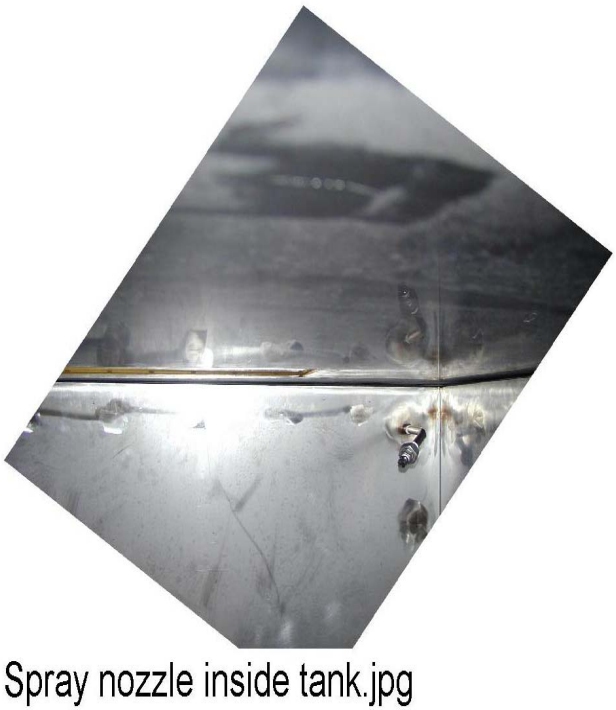

Figure 7. One of four spray nozzles located in each upper corner of the ICET tank. This photo was taken through the upper access hatch while the lid was in place.

Figure 8. The cover lid of the ICET tank showing the top observation window (lower) and top access hatch with handle (upper).

Figure 9 and Figure 10 present as-built dimensioned drawings of the tank and piping system from both the front and side views, respectively. Given that the tank system is oriented approximately along the standard geographic compass directions, the front view depicts the east face of the tank and the side view depicts the north face of the tank.

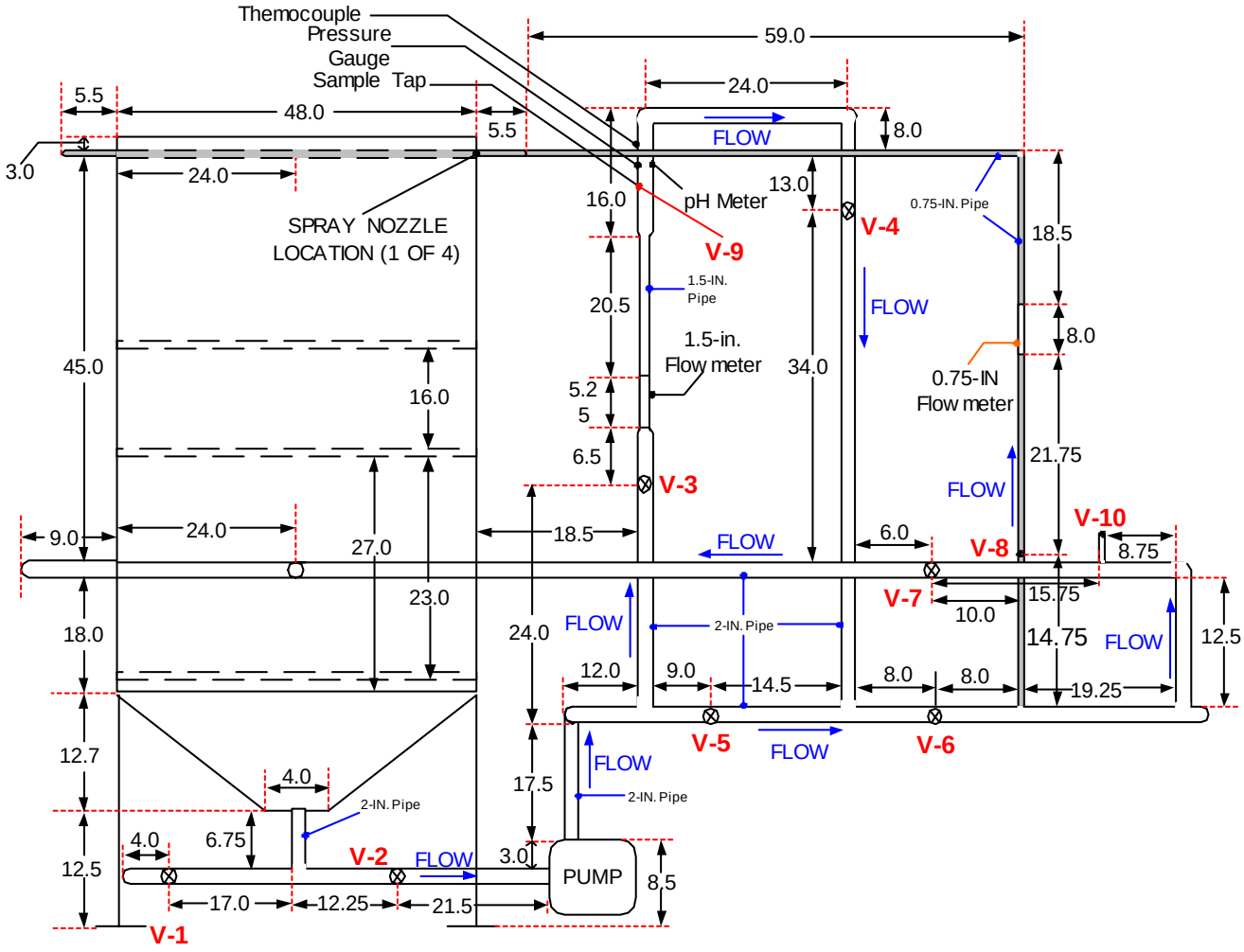

Figure 9. Front-view as-built dimensions of tank and piping system. Dimensions are in inches; shaded regions represent CPVC piping.

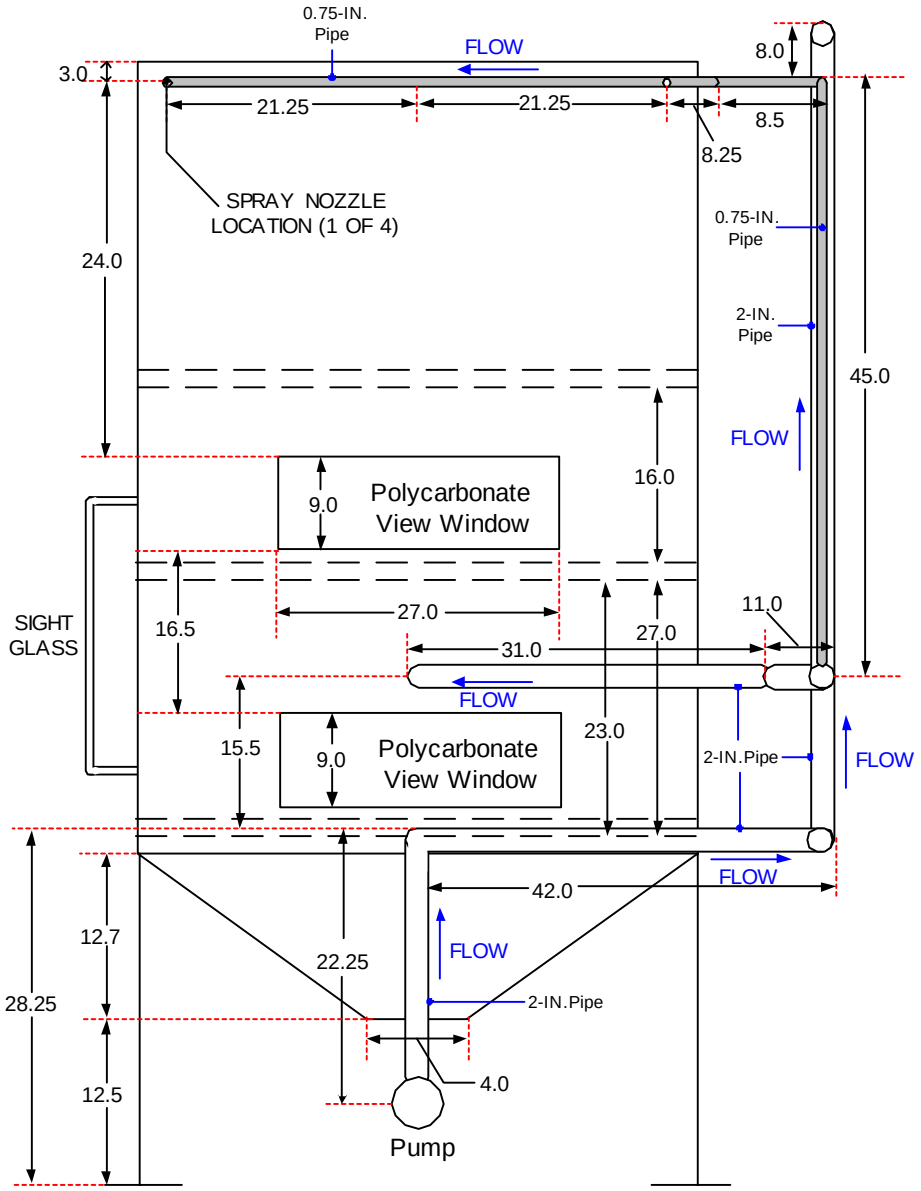

Figure 10. Side-view, as-built dimensions of tank and piping system. Dimensions are in inches; shaded regions represent CPVC piping.

3.2.3 Coupon Racks

The coupon racks are constructed of 1.5-in.-diam CPVC plastic piping. (see Figure 11). The racks prevent metal-to-metal contact between adjacent coupons and between the coupons and the rest of the tank assembly. This feature limits galvanic corrosion potential. Leaching tests were performed on the CPVC material and welding solvent to ensure that no detectable contributions to the chemical system would occur. Two complete sets of racks were built to facilitate staging of coupons for subsequent tests. The coupons can add up to 180 lb of weight to each CPVC-rack assembly. At elevated temperatures, the racks require support from 2-in.-wide SS angle irons strapped to the bottoms of the racks. These supports bridge the gap between the two sides of the tank and rest on the internal 2-in.-wide SS angle irons. A 16-

in. gap exists on each of the internal support angle irons to accommodate the lowering and emplacement of the nominal 14-in.-wide racks. The gap is then bridged with a length of angle iron that is pinned in place before the next tiers of racks are placed on top. See Figure 6 for the locations of the gaps and Figure 5 for an illustration of the short bridge angles.

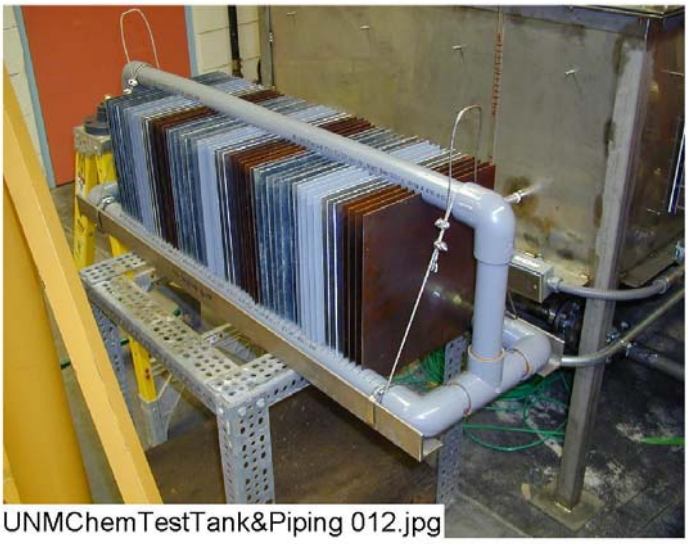

Figure 11. Photograph of a loaded coupon rack.

3.2.4 Tank Insulation

The tank is insulated with fiberglass boards. The surface area of the tank and top is approximately 130 ft^2. Approximately 50 linear feet of 2-in. diameter pipe remain uninsulated. The temperature of the fluid is nominally 140°F, and the outside surrounding air is approximately 70°F. The resulting heat loss from the tank and piping is approximately 1.2 kW.

3.2.5 Tank Heaters

The tank heaters are titanium jacketed to prevent corrosion and interaction of solution chemistry during the test series. Each heater is rated to supply 3.5 kW, thus providing excess (greater than the 1.2 kW required) redundant heating capacity and the ability to operate the tank assembly at higher temperatures if desired in the future. This additional capacity permits the convenience of having uninsulated piping runs. Under the existing electrical wiring configuration, only one heating element can be operated at a time. The locations of the two heaters inside the ICET tank are shown in Figure 5.

3.2.6 Pump Selection

The pump wetted parts are SS, and the seals are compatible with boric acid and sodium hydroxide solutions. The pump is sized to provide a flow rate of up to 100 gpm. The pump has a variable speed controller so that the desired flow can be achieved, regardless of the system head loss. Calculations of the desired velocities in the tank result in a nominal flow rate of approximately 25 gpm during test operation. A photograph of the pump selected for the ICET system is presented in Figure 12.

Figure 12. Circulation pump for the ICET system.

Each of the two injection flow headers, placed below the water line along the top of the submerged coupon rack, consists of a 1-in.-diam pipe with a symmetric pattern of holes to distribute the solution discharge. The desired flow velocity across the submerged coupons was accounted for, along with the desired loop flow rate and pump characteristics. The number and size of holes in the flow headers were calculated, and the holes were drilled symmetrically in each header. The primary goal of header design was to achieve a uniform flow pattern across the submerged coupons with velocities in the 0–3 cm/s range. During loop shakedown activities, plastic streamers were placed at various places in the tank to provide a visualization of the flow pattern. Then, the hole sizes were adjusted to achieve the desired pattern. Finally, food dye was introduced to determine the actual velocities. Tank velocities within the desired range were obtained.

The as-built configuration provides excess pressure head and flow capacity, even permitting for a doubling of the flow rate, if desired. A photograph showing one of the two parallel distribution headers is presented in Figure 5. One of the recirculation supply lines is shown in Figure 4 between the upper and lower observation windows.

3.3 Experimental Plan and Test Matrix

ICET test parameters were selected based on the results of surveys of U.S. nuclear power plants. Quantities of test materials were selected to preserve the scaling of representative ratios between material surface areas and total cooling-water volumes. Chemical additives also simulate the post-LOCA sump environment.

The materials included in the tests are zinc, aluminum, copper, carbon steel, concrete, and insulation materials, such as fiberglass and calcium silicate. The amounts of each material are given in Table 1 in the form of material-surface-areas to water-volume ratios, with the exceptions of concrete dust, which is presented as a mass to water-volume ratio, and fiberglass and calcium silicate, which are presented as insulation-volume to water-volume ratios. Also shown in the table are the percentages of the materials that are submerged and unsubmerged in the test chamber.

Table 1. Material Quantity/Sump Water Volume Ratios for the ICET Tests

Material	Value of Ratio for the Test (Ratio Units)	Percentage of Material Submerged (%)	Percentage of Material Unsubmerged (%)
Zinc in Galvanized Steel	8.0 (ft^2/ft^3)	5	95
Inorganic Zinc Primer Coating (Non-Top Coated)	4.6 (ft^2/ft^3)	4	96
Inorganic Zinc Primer Coating (Top Coated)	0.0 (ft^2/ft^3)	–	–
Aluminum	3.5 (ft^2/ft^3)	5	95
Copper (Including Cu-Ni alloys)	6.0 (ft^2/ft^3)	25	75
Carbon Steel	0.15 (ft^2/ft^3)	34	64
Concrete (Surface)	0.045 (ft^2/ft^3)	34	64
Concrete (Particulate)	0.0014 (lbm/ft^3)	100	0
Insulation Material (Fiberglass or Calcium Silicate)	0.137 (ft^3/ft^3)	75	25

The physical and chemical parameters, which are critical for defining the tank environment and have a significant effect on sump-flow blockage potential and gel formation, have been identified in Ref. 2. These physical and chemical parameters are summarized as follows.

Physical parameters:

Water volume in the test tank:	949 L	(250 gal.)
Circulation flow:	0-200 L/min	(0–50 gpm)
Spray flow:	0-100 L/min	(0–25 gpm)
Sump temperature:	60°C	(140°F)

Chemistry parameters:

H_3BO_3 concentration:	2800 mg/L as boron
$Na_3PO_4 \cdot 12H_2O$ concentration:	as required to reach pH 7 in the simulated sump fluid
NaOH concentration:	as required to reach pH 10 in the simulated sump fluid
HCl concentration:	100 mg/L
LiOH concentration:	0.7 mg/L as Li

The parameters planned for each ICET test run are described in Table 2.

Table 2. Test Series Parameters

Run	Temp (°C)	TSP $Na_3PO_4 \cdot 12H_2O$	NaOH	pH Target	Boron (ppm)	Note
1	60	N/A	Yes	10	2800	100% fiberglass insulation test. High pH, NaOH concentration, as required by pH (see Notes 2 and 3).
2	60	Yes	N/A	7	2800	100% fiberglass insulation test. Low pH, TSP concentration, as required by pH.
3	60	N/A	Yes	10	2800	80% calcium silicate/20% fiberglass insulation test. High pH, NaOH concentration, as required by pH (see Note 3).
4	60	Yes	N/A	7	2800	80% calcium silicate/20% fiberglass insulation test. Low pH, TSP concentration, as required by pH.
5	60	TBD	TBD	TBD	TBD	Confirmatory test; one of the above four tests will be repeated.

Notes:

1. The parameters in Table 2 are those presented in Reference 2, which was active when Test #1 was conducted. Subsequent revision of Reference 2 reversed the order of Tests #3 and #4.
2. The duration of Test #1 will be 30 days.
3. During the first 30 min of Tests #1 and #3, NaOH will be injected in the spray fluid.

   The quantity of NaOH injected in the spray solution is subject to the following constraints:

   a. The pH of the spray fluid shall not exceed a value of 12 during this initial 30-min injection phase; and

   b. The target pH of the simulated sump fluid inventory at the termination of the containment spray simulation (e.g., after the 30-min NaOH injection phase), not considering pH effects due to CO_2 absorption and other chemical effects that may be occurring during NaOH injection, is a value of pH = 10.

3.4 Analytical Methods

Data collected during Test #1 include the on-line measurements of temperature, pH, and loop flow rate. During the water grab sample analysis, bench-top measurements are obtained for temperature, pH, turbidity, total suspended solids (TSSs), and kinematic viscosity. Water, fiberglass, and metal samples are taken to other laboratory locations for additional analyses. These analyses include strain-rate viscosity, scanning electron microscopy (SEM), energy dispersive spectrometry (EDS), transmission electron microscopy (TEM), inductively coupled plasma mass spectrometry (ICP), x-ray fluorescence (XRF), and x-ray diffraction (XRD). Shear-rate viscosity is discussed in Section 4.5.6. The other analytical methods are described below.

3.4.1 Scanning Electron Microscopy (SEM)

The primary use of SEM is to study the surface topography of solid samples. The resolution of this technique is approximately two orders of magnitude better than optical microscopes and one order of magnitude less than TEM.[3] Scanning electron microscopy (SEM) was used to examine the precipitate from the Day-15 and Day-30 high-volume water samples.

3.4.1.1 Principle of Operation

An electron beam passing through an evacuated column is focused by electromagnetic lenses onto the specimen surface. The beam is then scanned over the specimen in synchrony with the beam of the cathode-ray display screen. The incident beam electrons (from the electron gun) do not simply reflect off the sample surface. As the beam travels through the sample, it can do three things: First, it can pass through the sample without colliding with any of the sample atoms (matter is mostly space). Second, it can collide with electrons from the sample atoms, creating secondary electrons. Third, it can collide with the nucleus of the sample atom, creating a backscattered electron.[4]

The incident beam is composed of highly energized electrons. If one of these electrons collides with a sample atom electron, an electron will be knocked out of its shell.

Figure 13[5] illustrates this action. The released electron is called a secondary electron and is weak in energy. If these secondary electrons are close enough to the sample surface, they can be collected to form an SEM image.

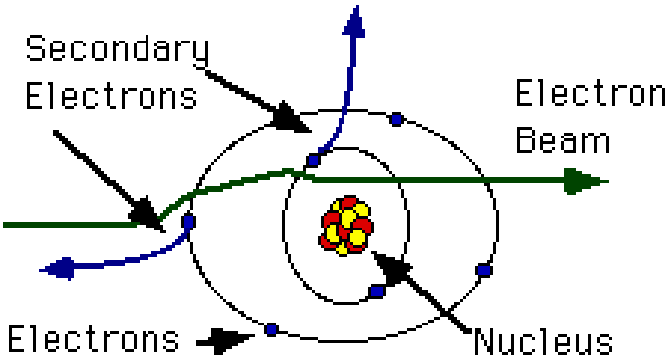

Figure 13. Production of secondary electrons from an electron beam.

The incident beam electron loses little energy in this collision. In fact, a single electron from the beam will produce a shower of thousands of secondary electrons until it does not have the energy to knock these electrons from their shells. Inelastically scattered secondary electron emission from the sample is used to modulate the brightness of the cathode ray display screen, thereby forming the image.

If the incident beam collides with a nucleus of a sample atom, it bounces back out of the sample as a backscattered electron (Figure 14).[6] These electrons have high energies, and because a sample with a higher density will create more of them, they are used to form backscattered electron images, which generally can discern the difference in sample densities. In this case, the image contrast is determined largely by compositional differences of the sample surface rather than by topographic features. Additional information on SEM may be found in Goldstein.[7]

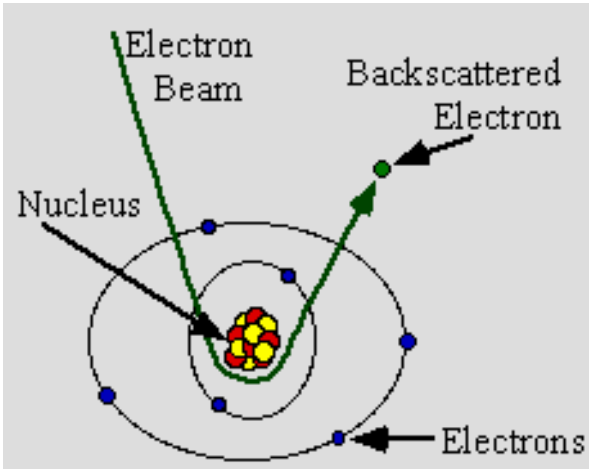

Figure 14. Production of backscattered electrons from an electron beam.

3.4.1.2 Limitations

The principle limitations of SEM are the resolution. Typical resolution is limited to between 1.5 and 3 nm, which is approximately an order of magnitude less than TEM.[8] In addition, only the surface of the specimen can be viewed. Finally, the SEM operates under high vacuum and therefore is unsuitable for examination of materials with a liquid component without suitable drying.

3.4.2 Energy Dispersive Spectroscopy (EDS)

EDS can provide information on the elemental composition of a specimen. Combining the EDS system with the SEM allows the microstructure-level identification of compositional gradients at grain boundaries, second phases, impurities, inclusions, and small amounts of material. EDS was used to examine the various structures formed on the fibers, which are similar for the Day-15 and Day-30 test samples. This examination allowed for a quantitative estimate of the elemental composition of the precipitate and the material deposited between the fibers.

3.4.2.1 Principle of Operation

As an incident electron beam interacts with the specimen, it loses energy. Characteristic x-rays are in turn emitted by the atomic species in the material. These characteristic x-rays are then converted into an electrical pulse with specific characteristics of amplitude and width. A multichannel analyzer measures the pulse and increments as a corresponding "energy slot" in a monitor display. The location of the slot is proportional to the energy of the x-ray photon entering the detector. The display is a histogram of the x-ray energy received by the detector, with individual "peaks," the heights of which are proportional to the amount of a particular element in the specimen being analyzed.[9] Additional information on EDS may be found in Goldstein.[10]

3.4.2.2 Limitations

The design of the equipment complicates the technique of detecting elements lighter than carbon. In general, a poorer sensitivity for light elements (low atomic weight) also exists in a heavy matrix. Resolution of the x-ray energy levels limits the positive identification of certain elements due to

overlapping energy slots. Quantitative analysis is usually limited to flat, polished specimens. Unusual geometries, such as fracture surfaces, individual particles, and films on substrates can be analyzed, but with considerably greater uncertainty.[11]

3.4.3 Transmission Electron Microscopy (TEM)

TEM is used to study the local structure, morphology, and chemistry of materials by examining the diffracted and transmitted electron intensities, as well as the characteristic x-rays and energies lost by the incident beam. TEMs are often coupled with EDS to give information about the local chemistry of the material. The high resolution of the transmission electron microscope (TEM), at least an order of magnitude greater than SEM, allows for qualitative size assessment of the underlying visible structures and aggregates. TEM was used on the precipitate from the 15-day and 30-day high volume samples.

3.4.3.1 Principle of Operation

In transmission electron microscopes, a beam of high-energy electrons, typically 100–400 KeV, is generated. The generated beam then is collimated by a magnetic lens and allowed to pass through the specimen under high vacuum. The resulting diffraction pattern, which consists of a transmitted beam and many diffracted beams, can be imaged on a fluorescent screen below the specimen. From the diffraction pattern, the lattice spacing information for the structure under consideration can be obtained. Alternatively, the transmitted beam or one of the diffracted beams can be used to form a magnified image of the sample. Finally, if the transmitted beam and one or more of the diffracted beams are allowed to recombine, a high-resolution image can be obtained that contains information about the atomic structure of the material.[12]

As the incident electron beam interacts with the specimen, it loses energy. Characteristic x-rays are in turn emitted by the atomic species in the material. These characteristic x-rays and the energy losses suffered by the incident electron then can be detected and analyzed to yield the EDS spectrum. Additional detail on TEM may be found in Williams.[13]

3.4.3.2 Limitations

A TEM can have extremely high resolution, and research-level instruments can see individual atoms. However, a TEM has some limitations because the electron beam must travel through the sample, and lengthy sample preparation is usually required to make the sample thin enough. Because the beam is traveling though the sample, the sample bulk, not the surface, is being imaged. [14]

3.4.4 Inductively Coupled Plasma by Atomic Emission Spectroscopy (ICP-AES)

ICP-AES is a rapid, sensitive way of measuring the elemental concentrations of solutions. More than 75 elements can be determined. ICP was used to determine the elemental composition of the daily water samples to assist in the overall understanding of the solution chemistry and corrosion behavior.

3.4.4.1 Principle of Operation

The first step in the procedure is conversion of the molecules in the sample to individual atoms and ions using a high-temperature, radio-frequency-induced argon plasma. The sample is introduced into the plasma as a solution. The sample is then pumped to a nebulizer, where it is converted to a fine spray and mixed with argon in a spray chamber. The purpose of the spray chamber is to ensure that only droplets in a narrow size range make it through into the plasma. Most of the sample drains away from the chamber; the rest is carried into the plasma and instantly excited by the high temperatures (5000–10,000 K). Atoms

become ionized with 99% efficiency. The excited elements emit photons that are detected by one or more photomultiplier tubes.[15] Additional information on ICP may be found in Montaser.[16]

3.4.4.2 Limitations

A notable limitation is the inability to measure hydrogen, carbon, nitrogen, and oxygen. In addition, silicon quantification is determined better by XRF because silicon will be lost to the vapor phase during ICP acid digestion procedures (as will certain trace elements, such as Hg, Se, As, and possibly Pb and Cd). The other notable disadvantage with the technique is that some minerals may not dissolve completely when employing the digestion procedure needed to use the ICP. Therefore, for samples containing substantial amounts of minerals (solids must be dissolved before analysis), XRF analysis is probably more appropriate for elemental determination. Interferences may also occur during ICP-AES due to overlap of the emission lines from the analyte and the interfering element and due to matrix effects. Finally, ICP is not suitable for determination of chemical speciation.[17]

3.4.5 X-Ray Fluorescence (XRF)

This x-ray technique is used to determine, both qualitatively and quantitatively, the elemental composition of a wide range of materials. XRF was used to examine the high volume water sample precipitate on days 15 and 30.

3.4.5.1 Principle of Operation

XRF is based on the photoelectric effect. When an atom is irradiated with highly energetic photons, an electron from one of the inner shells may be ejected (Figure 15). As the vacancy is filled by an electron from an outer shell, a photon is released, the energy of which is characteristic of the atom. This radiation is called fluorescent radiation, and each element has its own set of characteristic emission lines. The intensity and the energy of these lines are measured using a spectrometer that detects wavelength-dispersive XRF or energy-dispersive XRF.[18] Additional detail on XRF may be found in Jenkins.[19]

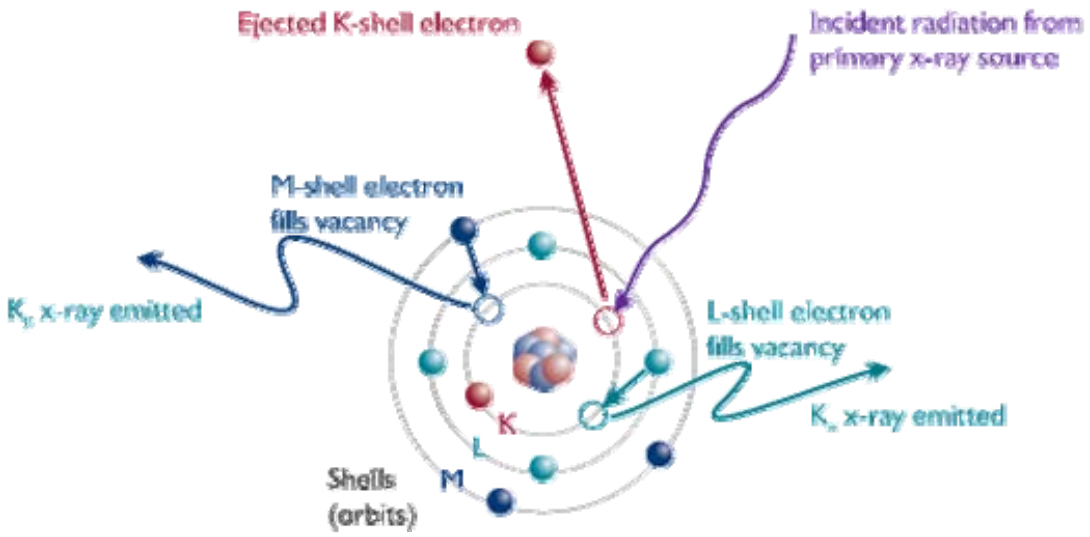

Figure 15. Illustration of the operation principle of XRF.

3.4.5.2 Limitations

The accuracy of the results depends on how closely the standards resemble the sample. In addition, the principle limitation with this technique is the decreased sensitivity that occurs with decreasing atomic weight. Most XRF instruments cannot reliably detect elements lighter than carbon. Another limitation is that for accurate quantitative analysis, standards that are similar in composition and morphology to the unknown are required.[20]

3.4.6 X-Ray Diffraction (XRD)

X-ray powder diffraction is used to obtain information about the structure, composition, and state of polycrystalline materials. The determination of the crystalline structure of the precipitate allows for the development of an understanding of the means by which the precipitate is formed. XRD analyses were performed on the post Test Sludge precipitate.

3.4.6.1 Principle of Operation

If a beam of monochromatic x-rays is directed at a crystalline material, reflection or diffraction of the x-rays is observed at various angles with respect to the primary beam. The relationship between the wavelength of the x-ray beam, λ, the angle of diffraction, 2θ, and the distance between each set of atomic planes of the crystal lattice, d, is given by the Bragg equation:

$$N\lambda = 2 d \sin\theta$$

where N represents the order of diffraction.

From this equation can be calculated the interplanar distances of the crystalline being studied. The interplanar spacing depends solely on the dimension of the crystal's unit cell, whereas the intensities of the diffracted rays are a function of the placement of the atoms in the unit cell.[21] Additional detail on XRD may be found in Barrett.[22]

3.4.6.2 Limitations

Conventionally, the largest limitation of XRD is its restriction to crystalline materials because amorphous materials do not diffract. Milligram samples may be analyzed if the analysis time is not important. The requirement of sample quantity (typically several hundred milligrams) is to provide the enormous number of small crystallites oriented in every conceivable direction. Thus, when an x-ray beam traverses the material, a significant number of the particles can be expected to be oriented to fulfill the Bragg condition for reflection from every conceivable interplanar spacing.

3.4.7 Wet Chemistry Analyses

The standard methods used for wet chemistry analyses are shown in Table 3. Additionally, the following paragraphs provide supplemental data for nonstandard methods and quality control practices.

Table 3. Methods for Chemical Analysis

Parameter	Method[a]	Major Equipment
pH	SM 4500-H^+ (Electrometeric)	Orion Model 720 A
Turbidity	SM 2130 (Nephelometeric)	Hach Turbidimeter Model 18900
Total Suspended Solids	SM 2540D	–
Temperature	SM-2550	–
Kinematic Viscosity	–	Cannon-Fenske Capillary Viscometer

[a]SM = Standard Methods for the Examination of Water and Wastewater (20th Edition) (APHA et al. 1998).

The pH meter was calibrated before use with a three-point calibration curve using certified pH buffers at 4, 7, and 10. An automatic temperature compensation pH probe was used to provide a temperature-corrected pH. The pH was recorded to the nearest 0.01 pH unit.

The turbidimeter was calibrated with Gelex secondary standards before testing. Turbidity was recorded to the nearest 0.01 Nephelometric Turbidity Unit (NTU).

For TSS, the glass fiber filters were weighed in aluminum boats for the pre-sample and post-sample weights. A standard volume of approximately 500 ml was filtered for all samples. The TSS was recorded to the nearest 0.1 mg/L.

3.4.7.1 Constant-Shear Kinematic Viscosity

Kinematic viscosity was measured with a Cannon-Fenske capillary viscometer. Viscosity was measured on both filtered and unfiltered samples, each at a temperature of 60 (±1.0)°C [140 (±1.8)°F] and again at 23 (±2.0)°C [73.4 (±3.6)°F]. The viscosity of water is highly sensitive to temperature, and the allowed temperature range results in a variation of viscosity of 2% between 59°C (138.2°F) and 61°C (141.8°F) and a 9.3% variation between 21°C (69.8°F) and 25°C (77.0°F). For this reason, temperature was measured to 0.1°C accuracy with a National-Institute-of-Standards-and-Technology-traceable thermometer for all viscosity measurements, and the measured viscosity values were corrected to a common temperature to facilitate comparisons. The corrected temperatures chosen for comparison were 60.0°C (140°F) and 23.0°C (73.4°F). Equations were derived to correct viscosity by fitting an equation to viscosity data and minimizing the coefficient of determination (R^2). The formulas used to correct the viscosity were

$$\nu_{23} = \nu_M \left(1.0235\right)^{(T_M - 23)}$$

and

$$\nu_{60} = \nu_M \left(1.0146\right)^{(T_M - 60)}$$

where

T_M = temperature at which viscosity measurements are made (°C),
ν_M = measured kinematic viscosity at temperature T_M (mm^2/s),
ν_{60} = kinematic viscosity corrected to 60.0°C (mm^2/s), and
ν_{23} = kinematic viscosity corrected to 23.0°C (mm^2/s).

In addition, duplicate measurements were made at each condition until Day 25 of the test. In nearly all cases, the replicate viscosity measurements varied by considerably less than 1%. On December 16, 2004, Day 25 of the test, duplicate measurements of viscosity were no longer taken because of the consistency previously noted.

3.5 QA Program

A project QA manual was developed to satisfy the contractual requirements that apply to the ICET Project. Specifically, those requirements were to maintain an appropriate level of QA in the areas of test loop design, sampling, chemicals, operation, and analysis to provide for credible results. These requirements were summarized in the contract requirement that QA was to be consistent with the intent of the appropriate sections of 10CFR50, Appendix B.

The 18 criteria of 10CFR50, Appendix B, were addressed separately in the QA manual, and the extents to which they apply to the ICET Project were delineated. A resultant set of QA procedures was developed. In addition, project-specific instructions were written to address specific operational topics that required detailed step-by-step guidance. Test #1 project instructions were written for the following topics:

- Data Acquisition System (DAS)
- Coupon Receipt, Preparation, Inspection, and Storage
- Pre-Test Operations
- Test Operations, Test #1 (NaOH at pH = 10)
- Chemical Sampling and Analysis
- Post-Test Operations
- DAS Alarm Response

All aspects of the ICET Project QA Program were reviewed and approved by the Project sponsors. Project personnel were trained in the QA manual, QA procedures, and project instructions.

3.5.1 ICP Quality Control

To ensure the accuracy of the ICP results, several QA analyses are performed with every batch of samples run on the instrument. The QA samples are as follows:

Lab Control Spike (LCS): The LCS consists of a known concentration of each analyte (typically 1 to 5 mg/L, depending on analyte) in deionized water. The measured concentration is compared with the spike concentration, and a percent recovery is reported. An exception is noted if the percent recovery of any analyte is outside of the acceptable range. The acceptable range is based on previous QA procedures developed for the instrument.

Method Blank (MB): The MB is a sample of deionized water. All analytes are expected to be below the detection limit. An exception is noted if the measured concentration of any analyte is above the detection limit.

Matrix Duplicate (MD): The MD is a second analysis of one of the samples in the run. The measured concentration for each analyte is compared between the two samples, and an exception is noted if the two results do not agree to within 20 percent.

Matrix Spike (MS): The MS consists of a known concentration of each analyte (typically 1 to 5 mg/L, depending on analyte) added to one of the samples in the run. The difference in the measured

concentrations between the original sample and spiked sample is compared with the spike concentration, and a percent recovery of the spiked concentration is reported. An exception is noted if the percent recovery of any analyte spike is outside of the acceptable range.

Matrix Spike Duplicate Accuracy (MSDA): The MSDA is a repetition of the MS. An exception on the MSDA is identical to an exception on the MS.

Matrix Spike Duplicate Precision: The two runs of the matrix spikes (MS and MSDA) are compared with each other. An exception is noted if the two measured spike concentrations do not agree to within a relative percent difference of 20 percent.

Serial Dilution: One of the samples in the run is diluted with deionized water by a factor of 5. The measured concentration of the diluted sample is compared with predicted concentration, which is calculated from the dilution rate and the measured concentration of the original (undiluted) sample. An exception is noted if the differences between the measured and calculated concentrations are not within the acceptable range.

It was necessary for the analytical laboratory to perform a 10:1 dilution of the samples to lower the concentration of borate to reduce interferences between borate and the analytes. This process had the effect of raising the detection limit for these analyses to a value 10 times higher than the instrument detection limit, but the higher detection limit had no impact on the results. The instrument detection limit was significantly below 1 mg/L for all analytes, and the higher detection limit was still well below the levels of concern for this experiment.

This page intentionally left blank.